Bootstrapping with Multi-frequency Mixed Code Carrier Linear Combinations and Partial Integer Decorrelation in the Presence of Biases

116

P. Henkel

Abstract

Carrier phase measurements are extremely accurate but ambiguous. The reliability of integer ambiguity resolution is improving with Galileo which uses a Binary Offset Carrier (BOC) modulation, large signal bandwidths of up to 50 MHz and additional carrier frequencies.

In this paper, a group of multi-frequency mixed code carrier linear combinations is derived which preserves geometry, eliminates the ionospheric delay and maximizes the ratio between wavelength and noise standard deviation of the combination. Moreover, a partial integer decorrelation is suggested to improve the robustness of ambiguity resolution over biases due to orbital errors, satellite clock offsets, and multipath.

The proposed group of multi-frequency mixed code carrier linear combinations is characterized by a wavelength of more than 3 m, which makes this group of combinations an interesting candidate for both Wide Area Real Time Kinematics (RTK) and Precise Point Positioning.

116.1 Introduction

Precise carrier phase positioning with Galileo and GPS requires the resolution of integer ambiguities. The reliability of ambiguity fixing can be improved by multi-frequency mixed code carrier linear combinations that eliminate the first order ionospheric delay, suppress the E1 code multipath by at least one order of magnitude, and maximize the ratio between wavelength and standard deviation of the combined noise.

P. Henkel (✉)
Institute of Communications and Navigation, Technische Universität München, Theresienstraße 90, 80333 München, Germany
e-mail: patrick.henkel@tum.de

A new ionosphere-free linear combination of Galileo E1, E5, E5a, E5b and E6 code and carrier phase measurements is derived that is characterized by a wavelength of 3.939 m and a noise level of a few centimeters for a carrier to noise power ratio of 45 dB-Hz. This combination also suppresses the E1 code multipath by 18.0 dB.

The integer ambiguities of the optimized linear combinations are fixed sequentially with bootstrapping (Blewitt 1989). An integer ambiguity transformation decorrelates the search space which improves the search efficiency dramatically but might result also in a substantial amplification of residual biases due to orbital errors, satellite clock offsets, and multipath. Therefore, a partial integer decorrelation is used for bootstrapping to achieve the optimum trade-off between variance reduction and bias amplification.

S. Kenyon et al. (eds.), *Geodesy for Planet Earth*, International Association of Geodesy Symposia 136,
DOI 10.1007/978-3-642-20338-1_116,

It is shown that the probability of wrong fixing can be reduced by up to 10 orders of magnitude compared to a complete integer decorrelation for phase biases of only 0.05 cycles. The partial integer decorrelation also improves the poor performance of integer least squares estimation techniques in the presence of biases.

Sequential ambiguity resolution based on multi-frequency mixed code carrier widelane combinations and partial integer decorrelation are considered to be an interesting candidate for both Precise Point Positioning and Wide Area RTK. These combinations increase the wavelength to several meters while the noise level is still kept at a centimeter level by carrier smoothing (Hatch 1982). The smoothing period can also be included in the combination design.

116.2 Derivation of Multi-frequency Code Carrier Linear Combinations

The carrier phase measurement on frequency $m \in \{1, \ldots, M\}$ at user $u = \{1, \ldots, U\}$ from satellite $k = \{1, \ldots, K\}$ is modeled as

$$\begin{aligned}\lambda_m \phi_{u,m}^k = {} & r_u^k + \delta r_u^k + c\left(\delta\tau_u - \delta\tau^k\right) \\ & - q_{1m}^2 I_u^k + T_u^k + \lambda_m N_{u,m}^k \\ & + b_{\phi_{u,m}}^k + \varepsilon_{\phi_{u,m}}^k, \end{aligned} \tag{116.1}$$

with the wavelength λ_m, the user-satellite range r_u^k, the projected orbital error δr_u^k, the user/satellite clock errors $\{c\delta\tau_u, c\delta\tau^k\}$, the ionospheric delay I_u^k on L1, the ratio of frequencies $q_{ij} = f_i/f_j$, the tropospheric delay T_u^k, the integer ambiguity $N_{u,m}^k$, the phase bias $b_{\phi_{u,m}}^k$ and carrier phase noise $\varepsilon_{\phi_{u,m}}^k$ including multipath. A similar model is used for the code measurements, i.e.,

$$\begin{aligned}\rho_{u,m}^k = {} & r_u^k + \delta r_u^k + c\left(\delta\tau_u - \delta\tau^k\right) \\ & + T_u^k + q_{1m}^2 I_u^k + b_{\rho_{u,m}}^k + \varepsilon_{\rho_{u,m}}^k. \end{aligned} \tag{116.2}$$

A multi-frequency mixed code carrier linear combination weights the phase measurements by α_m and the code measurements by β_m, i.e.,

$$\begin{aligned}\lambda\phi_u^k = {} & \sum_{m=1}^{M}\left(\alpha_m\lambda_m\phi_{u,m}^k + \beta_m\rho_{u,m}^k\right) \\ = {} & \sum_{m=1}^{M}(\alpha_m + \beta_m)\left(r_u^k + \delta r_u^k + T_u^k\right) \\ & + \sum_{m=1}^{M}(\alpha_m + \beta_m)\, c\left(\delta\tau_u - \delta\tau^k\right) \\ & + \sum_{m=1}^{M}\alpha_m\lambda_m N_{u,m}^k \\ & - \sum_{m=1}^{M}(\alpha_m - \beta_m)\, q_{1m}^2 \cdot I_u^k \\ & + \sum_{m=1}^{M}\left(\alpha_m b_{\phi_{u,m}}^k + \beta_m b_{\rho_{u,m}}^k\right) \\ & + \sum_{m=1}^{M}\left(\alpha_m\varepsilon_{\phi_{u,m}}^k + \beta_m\varepsilon_{\rho_{u,m}}^k\right). \end{aligned} \tag{116.3}$$

The linear combination preserves the range if

$$\sum_{m=1}^{M}(\alpha_m + \beta_m) = 1, \tag{116.4}$$

which preserves also the orbital error, the tropospheric delay and the clock offsets. A second constraint shall eliminate the ionospheric delay (IF constraint), i.e.,

$$\sum_{m=1}^{M}(\alpha_m - \beta_m)q_{1m}^2 = 0. \tag{116.5}$$

Moreover, the superposition of ambiguities should be an integer number of a common wavelength, i.e.,

$$\sum_{m=1}^{M}\alpha_m\lambda_m N_m = \lambda N, \tag{116.6}$$

which can be solved for N:

$$N = \sum_{m=1}^{M}\frac{\alpha_m\lambda_m}{\lambda}N_m \overset{!}{\in} \mathbb{Z}, \tag{116.7}$$

where $\mathbb{Z}$ denotes the set of integer numbers. Equation (116.7) is fulfilled if

$$j_m = \frac{\alpha_m \lambda_m}{\lambda} \overset{!}{\in} \mathbb{Z} \quad \forall m. \tag{116.8}$$

Solving for α_m yields

$$\alpha_m = \frac{j_m \lambda}{\lambda_m}. \tag{116.9}$$

The wavelength can be factorized into two components, i.e.,

$$\lambda = \tilde{\lambda}_0 \cdot w_\phi, \tag{116.10}$$

with

$$\tilde{\lambda}_0 = \frac{1}{\sum_{m=1}^{M} \frac{j_m}{\lambda_m}} \quad \text{and} \quad w_\phi = 1 - \sum_{m=1}^{M} \beta_m. \tag{116.11}$$

The $M + 2$ constraints of (116.4), (116.5) and (116.8) leave $M - 2$ degrees of freedom for the design of α_m and β_m. Therefore, a fourth constraint has been introduced by Henkel et al. (2009) to maximize the ambiguity discrimination, i.e.,

$$\max_{\substack{\alpha_1,\ldots,\alpha_M \\ \beta_1,\ldots,\beta_M}} D = \frac{\lambda(\alpha_1,\ldots,\alpha_M,\beta_1,\ldots,\beta_M)}{2\sigma_{\mathrm{n}}(\alpha_1,\ldots,\alpha_M,\beta_1,\ldots,\beta_M)}, \tag{116.12}$$

with

$$\sigma_{\mathrm{n}} = \sqrt{\sum_{m=1}^{M} \alpha_m^2 \sigma_{\phi_m}^2 + \sum_{m=1}^{M} \beta_m^2 \sigma_{\rho_m}^2}. \tag{116.13}$$

The optimization of (116.12) consists of a numerical search over j_m and an analytical computation of α_m and β_m which is presented here. The code weight β_2 is obtained from (116.4):

$$\beta_2 = 1 - \sum_{m=1}^{M} \alpha_m - \beta_1 - \sum_{m=3}^{M} \beta_m, \tag{116.14}$$

and the code weight β_1 is computed from the ionosphere-free constraint, i.e.,

$$\begin{aligned} \beta_1 &= \sum_{m=1}^{M} \alpha_m q_{1m}^2 - \sum_{m=2}^{M} \beta_m q_{1m}^2 \\ &= \sum_{m=1}^{M} \alpha_m q_{1m}^2 - \left(1 - \sum_{m=1}^{M} \alpha_m - \beta_1 - \sum_{m=3}^{M} \beta_m\right) q_{12}^2 \\ &\quad - \sum_{m=3}^{M} \beta_m q_{1m}^2. \end{aligned} \tag{116.15}$$

Replacing α_m by (116.9), using (116.10), and solving for β_1 yields

$$\beta_1 = s_1 + s_2 w_\phi + \sum_{m=3}^{M} s_m \beta_m, \tag{116.16}$$

with

$$s_1 = -\frac{q_{12}^2}{1 - q_{12}^2} \tag{116.17}$$

$$s_2 = \frac{\tilde{\lambda}}{1 - q_{12}^2} \cdot \sum_{m=1}^{M} \frac{j_m}{\lambda_m} \cdot (q_{12}^2 + q_{1m}^2) \tag{116.18}$$

$$s_m = \frac{q_{12}^2 - q_{1m}^2}{1 - q_{12}^2} \quad \forall m \in \{3,\ldots,M\}. \tag{116.19}$$

Equation (116.16) is used to rewrite (116.14) as

$$\beta_2 = 1 - s_1 - (1 + s_2) w_\phi - \sum_{m=3}^{M} (1 + s_m) \beta_m, \tag{116.20}$$

which allows us to express D as a function of w_ϕ and β_m, $m \geq 3$:

$$\begin{aligned} D = \frac{\tilde{\lambda}}{2} w_\phi \cdot \Bigg(& \tilde{\eta}^2 w_\phi^2 + \left(s_1 + s_2 w_\phi + \sum_{m=3}^{M} s_m \beta_m\right)^2 \sigma_{\rho_1}^2 \\ & + \left(1 - s_1 - (1 + s_2) w_\phi - \sum_{m=3}^{M} (1 + s_m) \beta_m\right)^2 \sigma_{\rho_2}^2 \\ & + \sum_{m=3}^{M} \beta_m^2 \sigma_{\rho_m}^2 \Bigg)^{-1/2} \end{aligned} \tag{116.21}$$

with $\tilde{\eta}^2 = \tilde{\lambda}^2 \cdot \sum_{m=1}^{M} \frac{j_m^2}{\lambda_m^2} \sigma_{\phi_m}^2$. The maximum discrimination is obtained by

$$\frac{\partial D}{\partial w_\phi} = 0, \tag{116.22}$$

and

$$\frac{\partial D}{\partial \beta_m} = 0 \quad \forall m \in \{3, \ldots, M\}. \tag{116.23}$$

Equation (116.23) is equivalent to

$$\begin{aligned} & s_m \sigma_{\rho_1}^2 \left(s_1 + s_2 w_\phi + \sum_{l=3}^{M} s_l \beta_l \right) - (1 + s_m) \\ & \cdot \sigma_{\rho_2}^2 \left(1 - s_1 - (1 + s_2) w_\phi - \sum_{l=3}^{M} (1 + s_l) \beta_l \right) \\ & + \beta_m \sigma_{\rho_m}^2 = 0, \end{aligned} \tag{116.24}$$

which can be written also in matrix-vector notation as

$$\boldsymbol{A} \cdot [\beta_3, \ldots, \beta_M]^T + \boldsymbol{b} \cdot w_\phi + c = 0, \tag{116.25}$$

with

$$\begin{aligned} \boldsymbol{A}_{m,l} &= s_l s_m \sigma_{\rho_1}^2 + (1 + s_l)(1 + s_m) \sigma_{\rho_2}^2 \\ &\quad + \sigma_{\rho_m}^2 \delta(m - l) \\ \boldsymbol{b}_m &= s_2 s_m \sigma_{\rho_1}^2 + (1 + s_m)(1 + s_2) \sigma_{\rho_2}^2 \\ \boldsymbol{c}_m &= s_1 s_m \sigma_{\rho_1}^2 - (1 + s_m)(1 - s_1) \sigma_{\rho_2}^2, \end{aligned} \tag{116.26}$$

and $\delta\ (m - l)$ being 1 for $m = l$ and 0 otherwise. Solving (116.25) for β_m yields

$$[\beta_3, \ldots, \beta_M]^T = -\boldsymbol{A}^{-1}(\boldsymbol{c} + \boldsymbol{b} \cdot w_\phi). \tag{116.27}$$

Constraint (116.22) is written in full terms as

$$\begin{aligned} & \left(s_1 + s_2 w_\phi + \sum_{m=3}^{M} s_m \beta_m \right) \cdot \left(s_1 + \sum_{m=3}^{M} s_m \beta_m \sigma_{\rho_1}^2 \right) \\ & + \left(1 - s_1 - (1 + s_2) w_\phi - \sum_{m=3}^{M} (1 + s_m) \beta_m \right) \\ & \cdot \left(1 - s_1 - \sum_{m=3}^{M} (1 + s_m) \beta_m \right) \sigma_{\rho_2}^2 + \sum_{m=3}^{M} \beta_m^2 \sigma_{\rho_m}^2 = 0. \end{aligned} \tag{116.28}$$

Replacing $[\beta_3, \ldots, \beta_M]^T$ by (116.27) yields

$$\begin{aligned} & \left(s_1 + s_2 w_\phi - \boldsymbol{t}^T \boldsymbol{A}^{-1} (\boldsymbol{c} + \boldsymbol{b} w_\phi) \right) \\ & \cdot \left(s_1 - \boldsymbol{t}^T \boldsymbol{A}^{-1} (\boldsymbol{c} + \boldsymbol{b} w_\phi) \right) \cdot \sigma_{\rho_1}^2 \\ & + \left(1 - s_1 - (1 + s_2) w_\phi + \boldsymbol{u}^T \boldsymbol{A}^{-1} (\boldsymbol{c} + \boldsymbol{b} w_\phi) \right) \\ & \cdot \left(1 - s_1 + \boldsymbol{u}^T \boldsymbol{A}^{-1} (\boldsymbol{c} + \boldsymbol{b} w_\phi) \right) \cdot \sigma_{\rho_2}^2 \\ & + (\boldsymbol{c} + \boldsymbol{b} w_\phi)^T \boldsymbol{A}^{-T} \boldsymbol{\Sigma} \boldsymbol{A}^{-1} (\boldsymbol{c} + \boldsymbol{b} w_\phi) = 0, \end{aligned} \tag{116.29}$$

with $\boldsymbol{t} = [s_3, \ldots, s_M]^T$, $\boldsymbol{u} = \boldsymbol{s} + \boldsymbol{1}$, and the diagonal matrix $\boldsymbol{\Sigma}$ that is given by

$$\Sigma = \begin{bmatrix} \sigma_{\rho_3}^2 & \boldsymbol{0} & 0 \\ \boldsymbol{0} & \ddots & \boldsymbol{0} \\ 0 & \boldsymbol{0} & \sigma_{\rho_M}^2 \end{bmatrix}. \tag{116.30}$$

(116.29) can be simplified as the quadratic terms with w_ϕ^2 cancel, i.e.,

$$r_1 + r_2 \cdot w_\phi = 0, \tag{116.31}$$

with

$$\begin{aligned} r_1 &= \left(s_1 - \boldsymbol{t}^T \boldsymbol{A}^{-1} \boldsymbol{c} \right)^2 \sigma_{\rho_1}^2 \\ &\quad + \left(1 - s_1 + \boldsymbol{u}^T \boldsymbol{A}^{-1} \boldsymbol{c} \right)^2 \sigma_{\rho_2}^2 \\ &\quad + \boldsymbol{c}^T \boldsymbol{A}^{-T} \boldsymbol{\Sigma} \boldsymbol{A}^{-1} \boldsymbol{c}, \end{aligned} \tag{116.32}$$

and

$$\begin{aligned} r_2 &= \left(\left(s_1 - \boldsymbol{t}^T \boldsymbol{A}^{-1} \boldsymbol{c} \right) \left(-\boldsymbol{t}^T \boldsymbol{A}^{-1} \boldsymbol{b} \right) \right. \\ &\quad \left. + \left(s_2 - \boldsymbol{t}^T \boldsymbol{A}^{-1} \boldsymbol{b} \right) \left(s_1 - \boldsymbol{t}^T \boldsymbol{A}^{-1} \boldsymbol{c} \right) \right) \cdot \sigma_{\rho_1}^2 \\ &\quad + \left(\left(1 - s_1 + \boldsymbol{u}^T \boldsymbol{A}^{-1} \boldsymbol{c} \right) \boldsymbol{u}^T \boldsymbol{A}^{-1} \boldsymbol{b} \right. \\ &\quad \left. - \left(1 + s_2 - \boldsymbol{u}^T \boldsymbol{A}^{-1} \boldsymbol{b} \right) \right. \\ &\quad \left. \cdot \left(1 - s_1 + \boldsymbol{u}^T \boldsymbol{A}^{-1} \boldsymbol{c} \right) \right) \cdot \sigma_{\rho_2}^2 \\ &\quad + \left(\boldsymbol{c}^T \boldsymbol{A}^{-T} \boldsymbol{\Sigma} \boldsymbol{A}^{-1} \boldsymbol{b} + \boldsymbol{b}^T \boldsymbol{A}^{-T} \boldsymbol{\Sigma} \boldsymbol{A}^{-1} \boldsymbol{c} \right). \end{aligned} \tag{116.33}$$

The optimum phase weighting $w_{\phi_{\text{opt}}} = -r_1/r_2$ is used in (116.27), (116.20) and (116.16) to obtain the code weights. (116.10) provides the optimum wavelength for the computation of the phase weights with (116.9).

The optimization of the multi-frequency linear combinations depends on the assumed phase and code noise variances. The latter ones are obtained from the Cramer Rao bound that is given by Kay (1993) as

$$\Gamma_m = \frac{c}{\sqrt{\frac{E_s}{N_0} \cdot \frac{\int (2\pi f)^2 |S_m(f)|^2 df}{\int |S_m(f)|^2 df}}}, \tag{116.34}$$

with the speed of light c, the signal to noise power ratio $\frac{E_s}{N_0}$, and the power spectral density $S_m(f)$ that has been derived by Betz (2001) for binary offset carrier (BOC) modulated signals. Table 116.1 shows the Cramer Rao lower bounds (CRB) of the Galileo signals of maximum bandwidth.

Table 116.2 shows the weighting coefficients and properties of multi-frequency linear combinations of maximum ambiguity discrimination. The dual frequency E1-E5a combination is characterized by a noise level of 31.4 cm and a wavelength of 4.309 m which allows reliable ambiguity resolution within a few epochs. As only the E1 and E5a frequencies lie in aeronautical bands, this linear combination might be useful for aviation. Linear combinations that comprise the wideband E5 and E6 code measurements benefit from a substantially lower noise level which turns into a larger ambiguity discrimination. It increases to 25.1 for the E1-E5 combination, to 39.2 for the E1-E5-E6 combination, and to 41.0 for the E1-E5a-E5b-E5-E6 combination. The large wavelength of these combinations makes them robust to the non-dispersive orbital errors and satellite clock offsets. The linear combination of measurements on 5 frequencies has the additional advantageous property of $|\beta_m| < 1$ and $|j_m| \leq 2$ for all m.

Table 116.1 CRB for $E_s/N_0 = 45$ dB–Hz

	Signal	BW [MHz]	Γ [cm]
E1	MBOC	20	11.14
E5	AltBOC(15,10)	51	1.95
E5a	BPSK(10)	20	7.83
E5b	BPSK(10)	20	7.83
E6	BOC(10,5)	40	2.41

116.3 Sequential Fixing with Partial Integer Decorrelation

The reliability of ambiguity resolution is increased by using two linear combinations: a code carrier combination of maximum discrimination and a code-only combination $\rho_u^k = \sum_{m=1}^{M} \tilde{\beta}_m \rho_{u,m}^k$. The weighting coefficients of the latter one are chosen to preserve geometry, eliminate the ionospheric delay, and to minimize the noise amplification. Both linear combinations are written in matrix vector notation for $U = 1$:

$$\begin{aligned} \boldsymbol{\Psi} &= \left[\lambda\phi_1^1, \ldots, \lambda\phi_1^K, \rho_1^1, \ldots, \rho_1^K\right]^T \\ &= \boldsymbol{H\xi} + \boldsymbol{AN} + \boldsymbol{n} + \boldsymbol{b}, \end{aligned} \tag{116.35}$$

Table 116.2 Geometry-preserving, ionosphere-free, integer-preserving mixed code carrier widelane combinations of maximum discrimination for $\sigma_\phi = 1$ mm and $\sigma_{\rho m} = \Gamma_m$

	E1	E5a	E5b	E5	E6	λ	σ_n	D
j_m	1			–1				
α_m	17.2629			–13.0593		3.285 m	6.5 cm	25.1
β_m	–0.0552			–3.1484				
j_m	1	–1						
α_m	22.6467	–16.9115				4.309 m	31.4 cm	6.9
β_m	–1.0227	–3.7125						
j_m	1	4	–5					
α_m	18.5565	55.4284	–71.0930			3.531 m	133.3 cm	13.3
β_m	–0.2342	–0.8502	–0.8075					
j_m	1			1	–2			
α_m	21.1223			15.9789	–34.2894	4.019 m	5.1 cm	39.2
β_m	–0.0200			–1.1422	–0.6495			
j_m	1	1	0		–2			
α_m	23.4845	17.5371	0.0000		–38.1242	4.469m	6.3cm	35.3
β_m	–0.0468	–0.1700	–0.1615		–1.5191			
j_m	1	1	0	0	–2			
α_m	20.6978	15.4562	0.0000	0.0000	–33.6004	3.938m	4.8cm	41.0
β_m	–0.0159	–0.0578	–0.0549	–0.9084	–0.5166			

with the geometry matrix $\boldsymbol{H}$, the unknown real-valued parameters $\boldsymbol{\xi} \in \mathbb{R}$, the wavelength matrix $\boldsymbol{A}$, the unknown integer ambiguities $\mathbf{N} \in \mathbb{Z}$, additive white Gaussian noise $\boldsymbol{n} \sim N(0, \Sigma)$ and biases $\boldsymbol{b}$. An integer least-squares estimator minimizes the weighted sum of squared errors, i.e.,

$$\min_{\xi, \boldsymbol{N}} \| \boldsymbol{\Psi} - \boldsymbol{H}\boldsymbol{\xi} - \boldsymbol{A}\boldsymbol{N} \|^2_{\Sigma^{-1}} \quad \text{s.t.} \quad \boldsymbol{N} \in \mathbb{Z}. \tag{116.36}$$

The least-squares float solution of ambiguities is obtained by an orthogonal projection and by disregarding the integer nature of ambiguities, i.e.,

$$\hat{\mathbf{N}} = \left(\bar{\boldsymbol{A}}^T \Sigma^{-1} \bar{\boldsymbol{A}}\right)^{-1} \bar{\boldsymbol{A}}^T \Sigma^{-1} \boldsymbol{\Psi}, \tag{116.37}$$

with

$$\bar{\boldsymbol{A}} = \boldsymbol{P}^{\perp}_{\boldsymbol{H}} \boldsymbol{A}, \tag{116.38}$$

and the orthogonal projection

$$\boldsymbol{P}^{\perp}_{H} = \boldsymbol{I} - \boldsymbol{P}_H = \boldsymbol{I} - \boldsymbol{H}(\boldsymbol{H}^T \Sigma^{-1} \boldsymbol{H})^{-1} \boldsymbol{H}^T \Sigma^{-1}. \tag{116.39}$$

The Least squares Ambiguity Decorrelation Adjustment (LAMBDA) method of Teunissen (1993) is in an integer least-squares estimator which uses an ambiguity transformation $\boldsymbol{Z}$ to decorrelate the search space space, and a search S for ambiguity fixing. The fixed ambiguity estimates are given by

$$\breve{\boldsymbol{N}} = \boldsymbol{Z}^{-1} S(\boldsymbol{Z}\boldsymbol{N}'), \tag{116.40}$$

where $\boldsymbol{Z}$ and S are described in details in Teunissen (1995) and Jonge and Tiberius (1996). An alternative integer estimation method is bootstrapping (Blewitt 1989) which fixes the float ambiguity estimates sequentially, i.e., the k-th conditional estimate is given by

$$\hat{N}_{k|1,\ldots,k-1} = \hat{N}_k - \sum_{j=1}^{k-1} \sigma_{\hat{N}_k \hat{N}_{j|1,\ldots j-1}} \sigma^{-2}_{\hat{N}_{j|1,\ldots j-1}} \cdot (\hat{N}_{j|1,\ldots j-1} - [\hat{N}_{j|1,\ldots j-1}]), \tag{116.41}$$

where [.] denotes the rounding operator and $\sigma^2_{\hat{N}_{j|1,\ldots j-1}}$ is the variance of the conditional ambiguity estimate. It is given by

$$\sigma^2_{\hat{N}_{k|1,\ldots,k-1}} = \sigma^2_{\hat{N}_k} - \sum_{j=1}^{k-1} \sigma^2_{\hat{N}_k \hat{N}_{j|1,\ldots j-1}} \sigma^{-2}_{\hat{N}_{j|1,\ldots j-1}}, \tag{116.42}$$

which depends on the order of fixings. This sequential fixing minimizes the variances of the conditional ambiguity estimates. These $\hat{N}_{k|1,\ldots,k-1}$ are uncorrelated, i.e.,

$$\sigma_{\hat{N}_{k|1,\ldots,k-1}, \hat{N}_{l|1,\ldots,l-1}} = 0 \quad \forall k \neq l. \tag{116.43}$$

Consequently, the success rate of ambiguity resolution can be computed analytically

$$P_{\mathrm{s}} = \prod_{k=1}^{K} \int_{-0.5}^{+0.5} \frac{1}{\sqrt{2\pi\sigma^2_{\hat{N}_{k|1,\ldots,k-1}}}} \cdot \exp\left(- \frac{(\hat{N}_{k|1,\ldots,k-1} - b_{\hat{N}_{k|1,\ldots,k-1}})^2}{2\sigma^2_{\hat{N}_{k|1,\ldots,k-1}}} \right) d\hat{N}_{k|1,\ldots,k-1}, \tag{116.44}$$

where $b_{\hat{N}_{k|1,\ldots,k-1}}$ denote the biases in the conditional ambiguity estimates (Teunissen 2001). The success rate of bootstrapping can be substantially improved by an integer ambiguity transformation $\boldsymbol{Z}$. This integer decorrelation transformation reduces the (co-) variances but also increases residual biases due to orbital errors, clock offsets and multipath. Therefore, a partial integer decorrelation with a reduced number L of decorrelation steps has been suggested by Henkel and Günther (2009), i.e.,

$$\boldsymbol{Z} = \boldsymbol{Z}^{(1)} \cdot \boldsymbol{Z}^{(2)} \cdot \ldots \cdot \boldsymbol{Z}^{(L)}, \tag{116.45}$$

where each $\boldsymbol{Z}^{(n)}$ includes an integer decorrelation $\boldsymbol{Z}^{(n)}_1$ and a permutation $\boldsymbol{Z}^{(n)}_2$ of two ambiguities, i.e.,

$$\boldsymbol{Z}^{(n)} = \boldsymbol{Z}^{(n)}_1 \cdot \boldsymbol{Z}^{(n)}_2. \tag{116.46}$$

116.4 Simulation Results

This section shows the benefit of multi-frequency mixed code carrier widelane combinations for Galileo. Simulated measurements are generated for the Galileo Walker constellation with 27 satellites. The section is

subdivided into two parts: First, double difference measurements are considered for Wide Area RTK (Hernandez-Pajares et al. 2000). The second subsection addresses Precise Point Positioning (Zumberge et al. 1997) with satellite–satellite single difference measurements.

116.4.1 Wide Area RTK

Double difference measurements are used to estimate the baseline (once per epoch), the integer ambiguities (with bootstrapping and integer decorrelation), the tropospheric wet zenith delay (of first epoch), the temporal gradient of the tropospheric wet zenith delay, the ionospheric delays for all satellites (of first epoch) and the temporal gradient of ionospheric delays for all satellites. The latter two parameters are not estimated in the case of IF combinations. The measurement noise is assumed to a follow a Gaussian distribution with the variances given by the Cramer Rao bounds of Table 116.1.

Figure 116.1 shows the benefit of the geometry-preserving, ionosphere-free E1-E5 code carrier combination of maximum ambiguity discrimination (Table 116.2) for ambiguity resolution. A geometry-preserving, ionosphere-free E1-E5 code-only combination is additionally used to exploit the redundancy of dual frequency measurements. The large wavelength of $\lambda = 3.285$ m reduces the probability of wrong fixing by more than 10 orders of magnitude compared to uncombined measurements with wavelengths of $\lambda_1 = 19.0$ cm and $\lambda_2 = 25.2$ cm. Measurements from only three epochs (separated by 1 s) were considered. The temporal variations in the probability of wrong fixing are caused by a change in the satellite geometry over 1 day as seen from our institute at 48.1507°N, 11.5690°E.

Figure 116.2 shows a comparison of different ambiguity resolution methods for both unbiased and biased measurements. The skyplot indicates the chosen satellite geometry with six visible satellites.

An ionosphere-free smoothing with smoothing time constant τ was applied to both the E1-E5 linear combination of maximum ambiguity discrimination and the E1-E5 code-only combination. The float ambiguity solution is then determined by least-squares estimation from the smoothed measurements of a single epoch. Obviously, a larger smoothing period results in a lower probability of wrong fixing. For unbiased measurements, the integer least-squares (ILS) estimation achieves the lowest error rate, followed by bootstrapping and rounding.

The SD bias amplitudes are modeled by an elevation dependent, exponential profile (horizon: 10 cm for code, 0.1 cycles for phase measurements; zenith: ten times lower values than in horizon) and the bias signs are chosen to obtain a worst-case bias accumulation over satellites and frequencies in the conditional ambiguities (Henkel and Günther 2009). Note that the bias amplitude is based on the satellite of lower elevation in the satellite–satellite SD pair, and that the

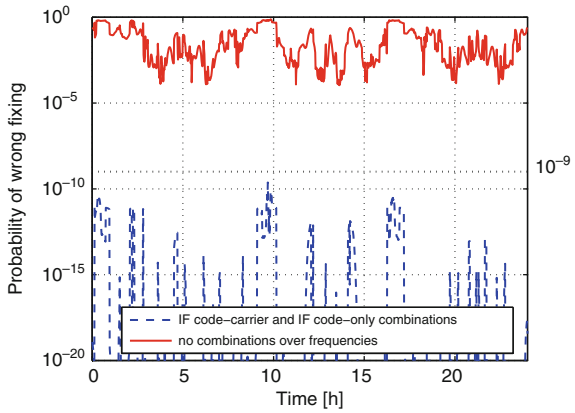

Fig. 116.1 Benefit of multi-frequency mixed code carrier linear combinations for ambiguity resolution: the increase in wavelength from 19.0 cm to 3.285 m enables a substantial reduction in the probability of wrong fixing

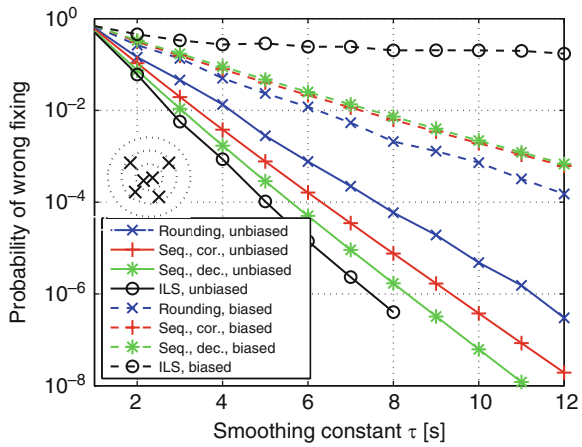

Fig. 116.2 Comparison of integer estimation methods for unbiased and biased measurements

satellite of highest elevation is chosen as reference satellite. Additionally, the Cramer Rao bounds are scaled by 3 to include multipath.

The optimality of the integer estimators is vice versa in the presence of worst-case biases, i.e., the integer ambiguity transformation results in an amplification of the biases which more than compensates for the gain obtained from the variance reduction. Note that the probabilities of wrong fixing for rounding and ILS were obtained from Monte Carlo simulations.

116.4.2 Precise Point Positioning

The optimized linear combinations of Table 116.2 are also beneficial for Precise Point Positioning (Zumberge et al. 1997) with satellite–satellite single difference measurements. The previously used E1–E5 code carrier and code-only combinations are smoothed over 10 s, and then used to estimate the receiver position (once per epoch), ambiguities and tropospheric zenith delay (once per epoch).

Figure 116.3 shows that an efficient integer search (LAMBDA) can be achieved either by the optimized code carrier combination with complete integer decorrelation, or by additionally using the code-only combination without integer decorrelation. Note that the first four ambiguities can always be fixed without frequent halted searches due to the four degrees of freedom for position and tropospheric wet zenith delay. However, the extremely low conditional variances of the 5th and further ambiguities result in frequent halted searches. The use of an integer decorrelation or of an additional linear combination flattens the ambiguity spectrum and, thereby, improves the search efficiency dramatically.

Figure 116.4 shows that a partial integer decorrelation with a reduced number of L decorrelation steps enables a substantial improvement in ambiguity fixing for worst-case SD phase biases of only 0.05 cycles (on both E1 and E5) in the horizon. The following assumptions were made for the remaining parameters of the elevation dependent, exponential SD bias profiles: zenith: 0.01 cycles for phase and 0.01 m for code biases; horizon: 0.05 m for code biases. A 30 s ionosphere-free smoothing was used to reduce the noise level and, thereby increase the margin for biases.

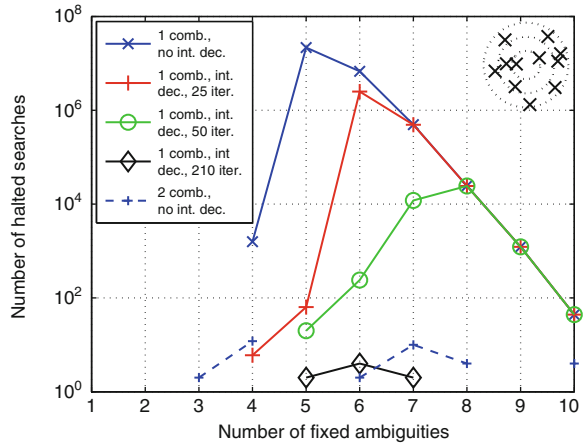

Fig. 116.3 Reduction of halted searches by multi-frequency linear combinations

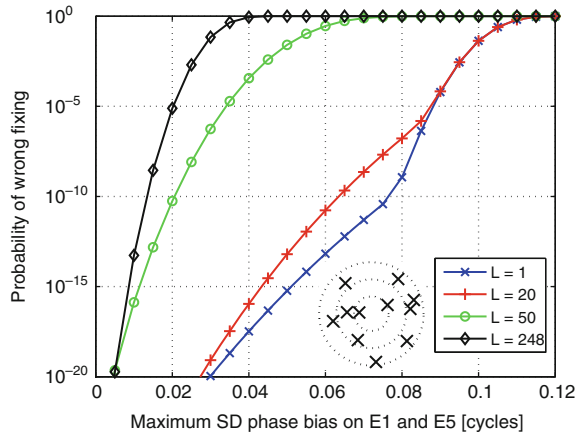

Fig. 116.4 Benefit of partial integer decorrelation for sequential ambiguity resolution

References

Betz J (2001) Binary offset carrier modulations for radionavigation. Navigation 48(4):227–246

Blewitt G (1989) Carrier-phase ambiguity resolution for the Global Positioning System applied to geodetic baselines up to 2000 km. J Geophys Res 94:10187–10203

Hatch R (1982) The synergism of GPS code and carrier phase measurements. Proceedings of the 3rd international geodetic symposium on satellite doppler positioning, vol 2, New Mexico, pp 1213–1232

Henkel P, Gomez V, Günther C (2009) Modified LAMBDA for absolute carrier phase positioning in the presence of biases. Proceedings of ION ITM, Anaheim, CA, pp 644–651

Henkel P, Günther C (2009) Partial integer decorrelation: optimum trade-off between variance reduction and bias amplification. J Geod 84:51–63

Hernandez-Pajares K, Juan J, Sanz J, Colombo O (2000) Application of ionospheric tomography to real-time GPS carrier-phase ambiguities resolution, at scales of 400–1000 km, and with high geomagnetic activity. Geophys Res Lett 27:2009–2012

Jonge P, Tiberius C (1996) The LAMBDA method for integer ambiguity estimation: implementation aspects, LGR Ser (12):1–59. TU Delft.

Kay S (1993) Fundamentals of statistical signal processing: estimation theory. Prentice Hall, Upper Saddle River, NJ, p 47

Teunissen P (1993) Least-squares estimation of the integer ambiguities. Invited lecture, Section IV, Theory and Methodology, IAG General Meeting, Beijing, China

Teunissen P (1995) The least-squares ambiguity decorrelation adjustment: a method for fast GPS integer ambiguity estimation. J Geod 70:65–82

Teunissen P (2001) Integer estimation in the presence of biases. J Geod 75:399–407

Zumberge J, Heflin M, Jefferson D, Watkins M, Webb F (1997) Precise point positioning for the efficient and robust analysis of GPS data from large networks. J Geophys Res 102: 5005–5017